

Spectroscopy of single atoms in the scanning tunneling microscope

N. D. Lang

IBM Thomas J. Watson Research Center, Yorktown Heights, New York 10598

(Received 9 June 1986)

A study is presented of the bias dependence of the tunneling current between two planar metal electrodes, each of which has an adsorbed atom. (One atom can be thought of as the tip, the other as the sample.) The positions of the peaks in a plot of the calculated $d \ln I / d \ln V$ versus V show a close correspondence to the positions of the resonances in the densities of states of both sample and tip.

We discuss here the extent to which spectroscopy in the scanning tunneling microscope¹⁻⁸ gives an accurate account of the surface-region density of states of the sample.^{9,10} For this purpose we study the vacuum tunneling current between two planar metallic electrodes as a function of the bias between them, in the instance in which there is a single adsorbed atom on each electrode.

The tunneling-Hamiltonian formalism¹¹ is used to calculate the total current in terms of the wave functions determined separately for each electrode in the absence of the other.¹² These wave functions are calculated starting with results on atomic chemisorption of Lang and Williams,¹³ as described in Ref. 14. The jellium model with $r_s = 2$ is used for each of the metal surfaces.

We describe our problem schematically as in Fig. 1. (We will employ atomic units in our discussion, in which $\hbar = m = |e| = 1$.) For the picture as shown, we define the current I and the bias V as positive. To simplify our discussion, we take the Fermi energy for the left electrode E_{FL} (measured with respect to the bottom of the conduction band for this electrode) to be equal to E_{FR} (the corresponding quantity for the right electrode): $E_{FL} = E_{FR} \equiv E_F$. Tunneling (for $V > 0$) takes place from filled states on the right with energy E_ν (measured with respect to the bottom of the conduction band on the right) to unfilled states on the left with energies $E_\mu = E_\nu + V$. The Hamiltonian for the left (right) electrode considered separately has eigenfunctions ψ_μ^L (ψ_ν^R), with eigenenergies E_μ (E_ν). The current at zero temperature is then

$$I = 4\pi \int d\mu \int d\nu [\theta(E_F - E_\nu) - \theta(E_F - E_\mu)] \times \delta(E_\mu - E_\nu - V) |J_{\nu\mu}|^2, \quad (1)$$

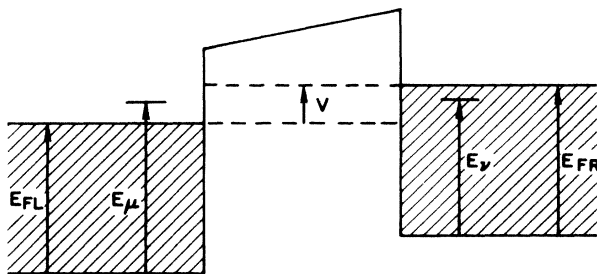


FIG. 1. Schematic diagram of energies in the tunneling problem.

where the step function $\theta(x)$ is 1 for $x > 0$ and 0 for $x < 0$,

$$J_{\nu\mu} = -\frac{1}{2}i \int dS \cdot [(\psi_\nu^R)^* \nabla \psi_\mu^L - \psi_\mu^L \nabla (\psi_\nu^R)^*], \quad (2)$$

and $\int d\mu$ ($\int d\nu$) is an integration over energy and a sum or integration over the other state labels as well. We do not extend the meaning of $\int d\mu$ ($\int d\nu$) to include a sum over both a stationary state and its complex conjugate as we did in Ref. 14 (it was necessary there in obtaining the current density), and so there is a factor of 4 in Eq. (1) that was not present in the analogous equation in that paper. The integral in Eq. (2) is over an infinitely extended surface in the vacuum region between the electrodes, as discussed in Ref. 11. Note that (given the δ -function restriction) the difference of step functions in Eq. (1) is nonzero only for energy levels in the strip of width V between the dashed lines in Fig. 1.

In this paper we will consider values of the bias, typically ~ 1 eV, that are relatively small on the scale of the work function, and we will therefore make the approximation of computing ψ_μ^L and ψ_ν^R in the absence of the electric field. We show our approximation schematically in Fig. 2 ($V > 0$ case) for ψ_μ^L , where the potential that slopes up into the vacuum region (dashed line) is replaced by a constant potential in this region (solid line). We make the corresponding approximation for ψ_ν^R , with the potential that slopes down into the vacuum region being replaced again by a constant potential.¹⁵ Thus ψ_μ^L will decay more slowly than it should in the vacuum region, while ψ_ν^R will decay more rapidly than it should, but if we evaluate Eq. (2) at the midpoint between the two electrodes, these two effects are seen (in a simple model calculation) to cancel

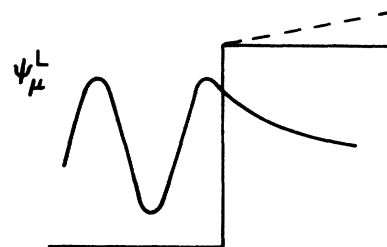


FIG. 2. Schematic representation of the approximation used in computing the wave functions.

to first order in the bias, leaving only a small second-order error.¹⁶

We will consider in our discussion a Na atom, which we label the tip, and a Ca atom, which we label the sample. (The present analysis however treats tip and sample entirely symmetrically.) Calculations for such systems, with a variety of lateral separations between tip and sample atoms, were given for the low-bias limit in Ref. 17. Here for simplicity we will consider just the case of zero lateral separation.¹⁸ We exclude from the calculated total current the current that would flow between the two bare metal surfaces in the absence of both atoms (which is infinite because of the infinite surface area); the result is nonetheless just denoted by I in our figures. (The current *density* in the absence of both atoms is $\sim 10^{-4}$ of the current density on the axis in the presence of the atoms.)

In Fig. 3 (top) we show the additional eigenstate density due to the presence of a Na atom and of a Ca atom on a metal surface, that is, the total eigenstate density for the metal-atom system, minus that of the bare metal. Note that the energy axis for Na (the top of the graph) is reversed for later convenience. In the case of Na, the fact that the resonance, which corresponds to the 3s valence level of the free atom, is mostly above the Fermi level indicates that the 3s electron of the Na has been largely lost to the metal. For Ca, the 4s valence shell of the free atom is filled, but in the adsorption case there is loss of electronic charge to the solid, with the result that the peak of the 4s resonance is near the Fermi level, as seen in the figure. Only the state density component with azimuthal quantum number $m=0$ (e.g., s and p_z) is shown, because $m \neq 0$ components make a much smaller contribution to the tunneling current for lateral separations that are not too large—cf. discussion in Ref. 14.

We now discuss the results of our calculations. The current is computed using Eq. (1) (much as it was computed in Ref. 17)¹⁹ for a number of values of the bias, and the results numerically differentiated to produce a table of dI/dV vs V . The center-to-center distance between the atoms is held fixed at 18 bohrs (9.5 Å), roughly the separation discussed in Ref. 17. We take the atom on the right to be the tip atom, and so by the convention of Fig. 1, positive bias represents tunneling from filled tip states to empty sample states, while negative bias represents tunneling from filled sample states to empty tip states. We plot $(dI/dV)/(I/V) = d \ln I / d \ln V$, as suggested by Feenstra, Stroscio, and Fein.⁸ (Note that this is unity for $V=0$.) These authors find experimentally that this dimensionless quantity is relatively independent of tip-sample separation, and that it gives a good account of the surface density of states of the sample.

The solid curve in Fig. 3 (bottom) gives $(dI/dV)/(I/V)$ for the case of a Ca atom on the left (sample) and a Na atom on the right (tip). The positions of the two Ca peaks and one Na peak in the density of states correspond reasonably well to the features of this curve. Note the negative values for V near +2 eV. Such “negative resistance” effects have been discussed by Esaki and Stiles.²⁰

In an experiment, it would be most convenient if the tip state density could be taken as relatively featureless, and thus be omitted from consideration. In at least one case

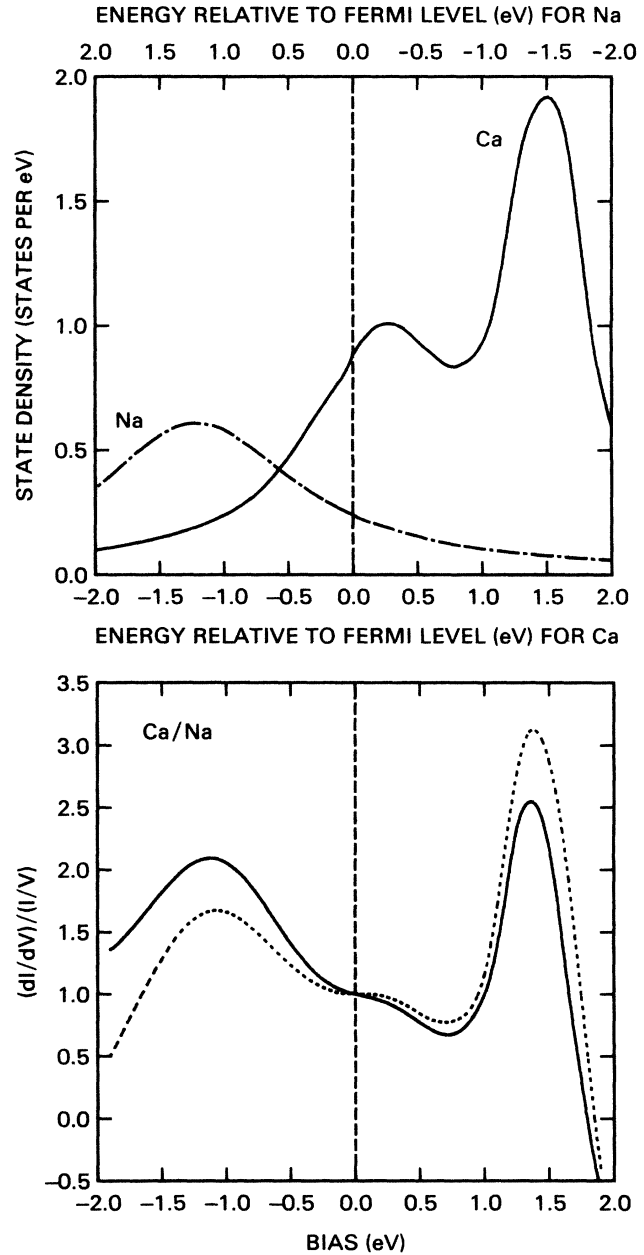


FIG. 3. Top: Curves of the difference in eigenstate density between the metal-atom system and the bare metal ($r_s=2$) for adsorbed Ca and Na. Note that the energy scale for Na (top) is reversed. The 3s resonance for Na is clearly evident. The lower-energy Ca peak corresponds to 4s, the upper to 3d (and some 4p). (Only $m=0$ is shown.) Bottom: solid line is calculated curve of $(dI/dV)/(I/V)$ vs V for Ca/Na; dotted line is same quantity evaluated using the simple model represented by Eq. (4).

(Ref. 8), tips were used which were purposely blunt (and probably disordered), and it was found that the tip state density appeared to play no significant role in the results. This seems quite reasonable, in view of the expectation that most of the sharp features in the density of states of such a tip would be washed out. Even if the tip were very sharp (a single atom), its state-density structure should be

similar to the often broad resonances in the cases studied here; it would certainly not exhibit the complex surface-state structure that may be characteristic of an extended ordered surface made of these same atoms.

Now let us discuss a rough approximation for the tunneling current in terms of the $m=0$ components of the state densities. By analogy with the results of Tersoff and Hamann²¹ for the low-bias limit, we expect crudely that^{3,22}

$$I \propto \int_{E_F}^{E_F+V} dE \rho_T(E-V) \rho_S(\mathbf{r}_T; E), \quad (3)$$

where $\rho_T(E)$ is the density of states associated with the tip atom (i.e., the total density of states for the metal-atom system minus that for the bare metal), which is taken to be on the right; $\rho_S(\mathbf{r}; E)$ is the local density of states due to the sample; and \mathbf{r}_T is the position of the center of the tip. Let us now say *roughly* that

$$\rho_S(\mathbf{r}_T; E) \propto \rho_S(E) e^{-2s\sqrt{2(W-E)+V}},$$

where $\rho_S(E)$ is the density of states associated with the sample atom, W is the height of the sample surface potential barrier (we think of it as square for simplicity), and s is the tip-sample separation. Again, we are taking only the $m=0$ components of all state densities (i.e., s and p_z for example, but not p_{xy}). This form would not be a very good approximation if there were a significant wave-vector parallel to the surface, since the decay length in that instance would be appreciably shorter, but cases of this type (e.g., certain surface states) do not occur in the present context. Note that we are using an "average barrier" approximation here.²³ (Note also that effects of current flow directly to or from the planar metal electrodes are omitted.) If we substitute this expression into Eq. (3), then we obtain, with a change of variable to emphasize the symmetry,

$$\begin{aligned} I &\propto \int_{E_F}^{E_F+V} dE \rho_T(E-V) \rho_S(E) e^{-2s\sqrt{2(W-E)+V}} \\ &= \int_{E_F-\frac{1}{2}V}^{E_F+\frac{1}{2}V} dE \rho_T(E-\frac{1}{2}V) \rho_S(E+\frac{1}{2}V) e^{-2s\sqrt{2(W-E)}}. \end{aligned} \quad (4)$$

(Note that $W=\Phi+E_F$, with Φ the work function.) This form is very convenient for discussion purposes. It is just an integral over the product of tip and sample state densities with the simplest barrier-penetration factor. When dI/dV is calculated using this form, in addition to products of state densities evaluated at the ends of the energy interval, there are terms associated with the V dependence of the integrand (which appear to be neglected in Ref. 3.)

The dotted curve in Fig. 3 (bottom) shows $(dI/dV)/(I/V)$ evaluated using Eq. (4) for the Ca-Na case.²⁴ The simple model provides a good account of the qualitative features of the results of the full calculation. Figure 4 (solid curve) shows what happens to $(dI/dV)/(I/V)$ in this model if we take the tip state density to be a constant, leaving the sample (Ca) state density unchanged. (The dotted curve is for both tip and sample state densities constant.) It is evident from this figure that for sufficiently negative bias, the Ca atom would be essentially invisible, because its state density has no structure in the corresponding energy region.

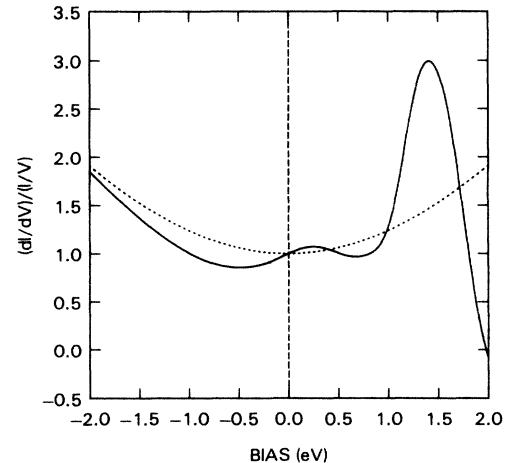


FIG. 4. Solid line: obtained using Eq. (4) with Ca sample and constant-state-density tip. Dotted line: obtained using Eq. (4) with constant-state-density tip and sample.

We can investigate the comparative utility of curves of $(dI/dV)/(I/V)$ and dI/dV in a simple way by taking the tip state density in Eq. (4) to be constant and the sample state density to be a Lorentzian (see Fig. 5). For the case of such a peak centered, e.g., 1 eV above the Fermi level (and a 4-eV work function and separation s equal to that used above²⁴), we graph the deviation from the Lorentzian center of the positions of the peaks in $(dI/dV)/(I/V)$ and dI/dV , as a function of the Lorentzian peak width. We see that over the range shown, the maximum deviation for dI/dV is three times what it is for $(dI/dV)/(I/V)$. This, of course, depends on the presence of the barrier penetration factor. If it were not included, there would be no shift of the peak in dI/dV away from the peak in the Lorentzian, but a shift would remain for $(dI/dV)/(I/V)$.

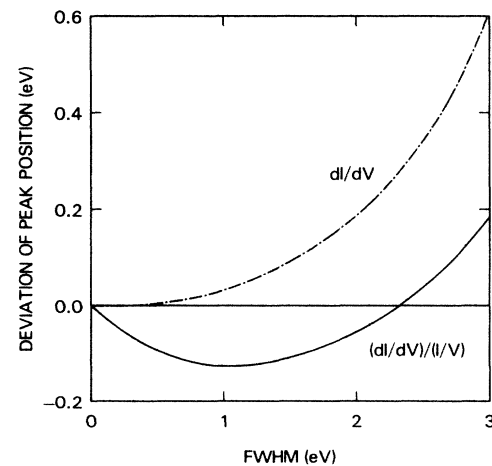


FIG. 5. Results calculated using Eq. (4) with constant-state-density tip and Lorentzian-state-density sample. Solid line: difference between position of peak in $(dI/dV)/(I/V)$ and position of peak in Lorentzian, as a function of full width at half maximum (FWHM) of Lorentzian. Dot-dash line: same for dI/dV .

I am delighted to thank R. M. Feenstra, J. Tersoff, A. R. Williams, J. E. Demuth, and R. M. Tromp for their comments on the manuscript.

- ¹G. Binnig, K. H. Frank, H. Fuchs, N. Garcia, B. Reihl, H. Rohrer, F. Salvan, and A. R. Williams, *Phys. Rev. Lett.* **55**, 991 (1985).
- ²R. S. Becker, J. A. Golovchenko, D. R. Hamann, and B. S. Swartzentruber, *Phys. Rev. Lett.* **55**, 2032 (1985).
- ³A. Selloni, P. Carnevali, E. Tosatti, and C. D. Chen, *Phys. Rev. B* **31**, 2602 (1985).
- ⁴G. Binnig, H. Fuchs, Ch. Gerber, H. Rohrer, E. Stoll, and E. Tosatti, *Europhys. Lett.* **1**, 31 (1986).
- ⁵R. M. Feenstra, W. A. Thompson, and A. P. Fein, *Phys. Rev. Lett.* **56**, 608 (1986).
- ⁶R. J. Hamers, R. M. Tromp, and J. E. Demuth, *Phys. Rev. Lett.* **56**, 1972 (1986).
- ⁷W. J. Kaiser and R. C. Jaklevic, *IBM J. Res. Dev.* **30**, 411 (1986).
- ⁸R. M. Feenstra, J. A. Stroscio, and A. P. Fein (unpublished).
- ⁹D. Penn, R. Gomer, and M. H. Cohen, *Phys. Rev. B* **5**, 768 (1972); D. R. Penn and E. W. Plummer, *ibid.* **9**, 1216 (1974).
- ¹⁰Cf. also, J. A. Appelbaum and W. F. Brinkman, *Phys. Rev. B* **2**, 907 (1970).
- ¹¹J. Bardeen, *Phys. Rev. Lett.* **6**, 57 (1961).
- ¹²All image effects are omitted.
- ¹³N. D. Lang and A. R. Williams, *Phys. Rev. B* **18**, 616 (1978); *Phys. Rev. Lett.* **37**, 212 (1976).
- ¹⁴N. D. Lang, *Phys. Rev. Lett.* **55**, 230 (1985); **55**, 2925 (1985); *IBM J. Res. Dev.* **30**, 374 (1986).
- ¹⁵This would, of course, not be appropriate for a bias large enough to give rise to oscillatory behavior of the wave function in a region between the two electrodes.
- ¹⁶To estimate this error, imagine that we consider tunneling for a one-dimensional problem where the barrier configuration is actually the one given in Fig. 1. Take the step barriers on either side to have the same height W , and for the positive bias shown, define $\xi = W - E_v$. (For negative bias, we would define $\xi = W - E_\mu$.) Note that in the calculation $\xi \geq \Phi$, the work function. We now determine ψ_μ^L and ψ_v^R for the actual sloping

barriers in terms of Airy functions (in the barrier region), and for the constant barriers in terms of exponentials. If we call s the width of the barrier region, and consider $E_\mu = E_v + V$, then for small V/Φ and for the range of separation distances and work functions relevant in the experiments,

$$\frac{|J_{v\mu}|^2}{|J_{v\mu}^{\text{approx}}|^2} \approx 1 - \left(\frac{s\sqrt{2\xi}}{24} + \gamma \right) \frac{V^2}{\xi^2},$$

where γ represents a rather complicated expression whose value is $\lesssim 0.05$ for cases of interest to us. For $V \sim 1$ eV, $\xi \geq \Phi \sim 4$ eV, and $s \sim 12$ bohrs (6 Å), our approximation represents an error in $|J_{v\mu}|^2$ of $\sim 2\%$.

- ¹⁷N. D. Lang, *Phys. Rev. Lett.* **56**, 1164 (1986).
- ¹⁸In this case, tunneling between the atoms is much more important than from an atom to the opposite metal surface, and we will thus, for convenience, not subtract from the calculated current that due to tunneling from the sample atom to the surface on which the tip atom is located as we did in Ref. 17.
- ¹⁹For computational efficiency, we only include wave functions with $m=0$ in our calculation, which is entirely adequate for small values of the lateral separation.
- ²⁰L. Esaki and P. J. Stiles, *Phys. Rev. Lett.* **16**, 1108 (1966).
- ²¹J. Tersoff and D. R. Hamann, *Phys. Rev. Lett.* **50**, 1998 (1983); *Phys. Rev. B* **31**, 805 (1985).
- ²²The actual argument given in Ref. 21 for an s -wave tip does not go through exactly for the case of nonzero bias, but the rough argument used there for discussion purposes in which the tip is replaced by a point probe can be used.
- ²³Cf. E. L. Wolf, *Principles of Electron Tunneling Spectroscopy* (Oxford, New York, 1985), p. 34.
- ²⁴We take s to be the distance between the nominally defined outer shells of the atoms on the opposite electrodes. This is ~ 12 bohrs in the present case, where the center-to-center distance is 18 bohrs. The exact value is not very important however.